INSTITUTE OF PHYSICS PUBLISHING MODELLING AND SIMULATION IN MATERIALS SCIENCE AND ENGINEERING

Modelling Simul. Mater. Sci. Eng. **13** (2005) 389–399 doi:10.1088/0965-0393/13/3/008

Monte Carlo simulation of linear aggregate formation from CdTe nanoparticles

A Sinyagin[1,5], **A Belov**[1,2] **and N Kotov**[1,3,4]

[1] Department of Chemical Engineering, University of Michigan, Ann Arbor, MI 48109, USA
[2] Karpov Institute of Physical Chemistry (NIFHI), Moscow, 103064, Russia
[3] Department of Materials Science, University of Michigan, Ann Arbor, MI 48109, USA
[4] Department of Biomedical Engineering, University of Michigan, Ann Arbor, MI 48109, USA

E-mail: sau@umich.edu

Received 28 October 2004, in final form 11 February 2005
Published 21 March 2005
Online at stacks.iop.org/MSMSE/13/389

Abstract

In recent works it was found that nanometre sized particles of CdTe could spontaneously reorganize into crystalline nanowires (NWs) upon controlled removal of the protecting shell of organic stabilizer in an aqueous medium. At present, there is no possibility of predicting for certain the outcome of each particular NW self-assembly experiment or influencing the geometric parameters of the aggregates. A model for the simulation of the interaction of CdTe nanoparticles (NPs) and their aggregation into clusters has been developed and a Monte Carlo simulation was performed. A 'linearity coefficient' has been developed and introduced into the model that allows for the comparison of NP aggregate geometries and investigation of the dependence of aggregate shapes on NP charge and dipole strength. The simulation results show that the presence of a dipole moment is crucial to the formation of chain-like NP aggregates. The shapes of the clusters that were obtained during simulations resemble those seen in the experiment, although serious differences are still observed, which hint at the influence of other, most probably, short-range interparticle forces on the clustering process.

1. Introduction

Low-dimensional species of semiconductor materials, such as nanoparticles (NPs), nanowires (NWs) and quantum wells, have been widely studied in recent years. The interest in quantum-confined structures is fuelled by the many possibilities of using their size-tunable optical and electrical properties in a new generation of optoelectronic devices [1–5]. At the present time, many different methods for the synthesis of NPs [5–7] and NWs are available.

[5] Author to whom any correspondence should be addressed.

The two major approaches are the gas-phase methods, such as vapour–liquid–solid (VLS), and the solution/liquid phase synthesis. The advantages of the solution-based synthesis include relatively lower reaction temperatures and precise control over the dimensions of the NPs. Liquid phase NW synthesis methods have been developed for a wide range of semiconductors [8–12]. A simple and versatile method for the synthesis of CdTe NWs by means of a spontaneous organization of single NPs was shown recently [13, 14]. Here, the removal of some of the organic stabilizer induced the formation of pearl-necklace aggregates, which subsequently recrystallized into NWs with a high aspect ratio and a diameter precisely defined by the starting NPs. However, at the present stage, there is no possibility of predicting with certainty the outcome of each particular NW self-assembly experiment or influencing the geometric parameters of the aggregates, because the exact mechanism of NW formation is as yet unknown. A prime candidate for the driving force behind the self-organization process is the dipole–dipole interaction of the particles. II–VI semiconductor NPs in both hexagonal and cubic crystal structures were, experimentally found to possess significant dipole moments [15, 16]. Whether these dipole moments are intrinsic to the NPs, or are the results of charged defects and other causes, is still a matter of debate [16–18]. In any case, the existence of a dipole moment will influence the aggregation of the NPs, since dipole–dipole interactions could be, by far, larger than the Van der Waals interaction at intermediate particle separations [19]. The mutual electrostatic repulsion of the NPs, which counters the dipole–dipole attraction, is provided by the stabilizer shell and decreases with decreasing stabilizer concentration. This process further enhances dipole–dipole interaction of the NPs. At the same time, the formation of pearl-necklace agglomerates was observed for metal NPs in solution [20, 21]. For these materials, the origin of the dipole moment is not quite as understandable as for the wurtzite semiconductor NPs and different explanations for the aggregation have been proposed. Additionally, the formation of the NP chains of CdTe NPs is observed in aqueous media, while dipole attraction can potentially be substantially stronger in organic media due to lower dielectric constants.

Since spontaneous self-organization of NPs [13, 22–27] usually involves millions of colloidal particles, any theoretical description of it needs to have substantial statistical accuracy. The most convenient method of calculation of the spatial arrangement of a large ensemble of particles, taking into account spontaneity and the random character of individual assembly steps, is computer simulation. Monte Carlo (MC) modelling methods are widely used in research, including in the simulation of nanocolloid chemical potentials and pair potentials between dipolar proteins or colloids [28–31]. Because of their stochastic nature, MC methods are frequently applied for treating equilibrium self-assembled structures such as self-assembled polymers and equilibrium polymerization [32, 33], electrostatically directed self-assembly [34], assembly of bis-biotinylated DNA and streptavidin [35] and others. Previous computer simulation of colloidal systems showed that the attractive interaction potential between colloidal macro-ions with a net dipole moment in ionic solution strongly increases at short distances and may overweigh the charge–charge repulsion at relevant separations [28–30].

Thus, a model that would describe the interaction of the NPs in solution during aggregation, taking into account all possible forces acting between NPs and providing the correlation between NP properties, aggregation procedure parameters (solvent type, temperature, concentration, etc) and final aggregate and NW geometry, would, on the one hand, provide a definitive answer about what forces cause this interesting and potentially useful phenomenon, and, on the other hand, help determine whether a synthesis of aggregates of predesigned geometrical layouts would be possible and which parameters would have to be controlled in order to achieve that. From this point of view, the need of quantitative evaluation,

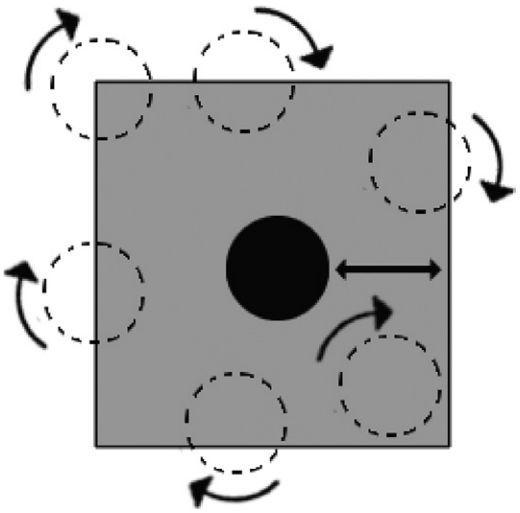

Figure 1. Implementation of classical MC moves for NP diffusion.

which would allow us to compare the system configurations from different simulation runs and its affinity to the line, becomes a necessity. Such a quantitative parameter would also allow us to compare simulation data with experimental results.

MC simulations of systems consisting of a number of particles interacting in water were carried out to estimate the degree of influence of the dipole moment of the individual NPs on the patterns of their aggregation. The simulation results show that, indeed, the presence of a dipole moment is crucial to the formation of chain-like NP aggregates. The shapes of the clusters that were obtained during simulations resemble those seen in the experiment [13, 14], although serious differences are still observed, which hint at the influence of other, most probably, short-range interparticle forces on the clustering process.

2. Modelling

2.1. Simulation method

The NVT MC method was used to obtain the equilibrium geometric configuration of the system. At the beginning of the simulation the particles were arranged randomly within the simulation box. During each step of the simulation, the particles were either randomly rotated around the X, Y and Z axes or moved by a random walk procedure $r_i(s_{n+1}) = r_i(s_n) + \xi_i$, $i = 1, \ldots, N$, where $\xi_i(x, y, z)$ was obtained from a Gauss distribution in accordance with the prescriptions of the random number generator on the basis of the previous configuration and the diffusion coefficient for the assigned environment parameters (figure 1). Every new arrangement of the particles was accepted or rejected according to the Metropolis criteria [36], with the probability determined by the Boltzmann distribution factor. From thermodynamical considerations, we would expect the global energy minimum of the system to correspond to a hexagonal close-packed array of particles, but, since we know that stable particle aggregates of various shapes are formed experimentally [13] our present goal was to find local minima that they match.

It is a known fact that classical MC methods become less efficient when used for simulation of particles aggregating into clusters [37–40]. The strong interaction of the particles dramatically inhibits the mobility of the clusters because it is dependent on the number of

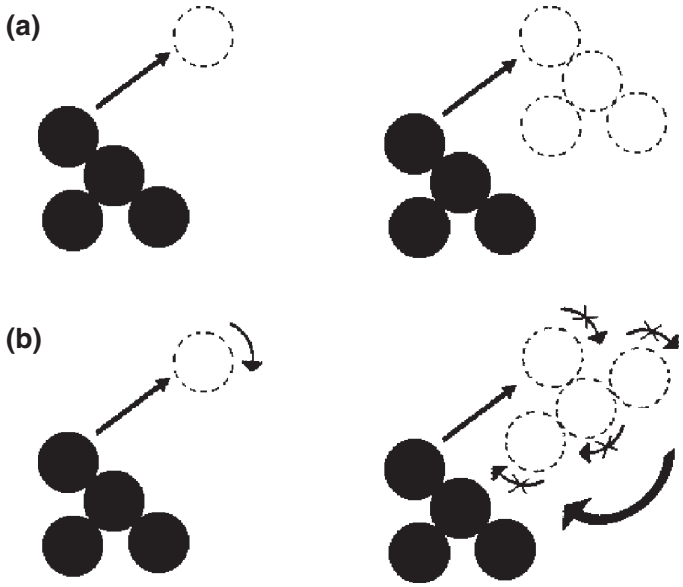

Figure 2. Translational (*a*) and rotational (*b*) movement of a NP cluster.

particles in the cluster and, therefore, the majority of the steps, where any one of the constituents tries to move away from the group, are rejected [40]. This leads to the situation where only individual particles or dimers have any mobility in the system, the larger aggregates being confined to the spot where they were formed. To reduce the number of steps with zero probabilities and avoid the confinement of the system to a global minimum, the method above was slightly modified. An aggregate, or cluster A, was formed at any stage of the simulation if

$$\forall i \in A, \exists k \in A : d(i,k) < \varepsilon_0, \tag{1}$$

which means that for any particle within the cluster there exists at least one particle from the same cluster with the centre-to-centre distance less than $\varepsilon_0 = R + \delta$, where R is the radius. Then particles were assigned to a 'group' and from that moment forth the group was moved or randomly rotated around the centre of mass, with the relative positions of the particles in the group intact, as seen in figure 2. This method generates an equilibrium configuration of the system with a finite number of simulation steps and meets the detailed balance conditions due to the separation of the rotation and translation steps, as well as step inversity. The above-mentioned cluster (group) assignment procedure was implemented using a recursive algorithm based on equation (1) during each step of the simulation. The particle interaction modelling process employed two- and three-dimensional systems, which consisted of up to 600 CdTe NPs with diameters $d = 1.5$–5.5 nm. CdTe nanocrystals have a cubic zinc blended structure and TEM images of the experimentally observed pearl-necklace aggregates show the shape of the NPs to be spherical [13]; therefore, each NP was approximated by a solid sphere with a permanent dipole moment and a net charge located at the centre of the particle. The magnitude of the dipole and net charge varied during different simulation runs. The experimental values of dipole moments for II–VI type semiconductor NPs like CdTe lie in the range of 20–100 D [16]. The simulation showed that the system of 20 particles reaches relative energy balance condition after $\sim 10^5$ MC steps.

2.2. Force field

The simulation force field was based on the classical DLVO theory, which takes into account only the electrostatic and Van der Waals dispersion interactions of the NPs [41, 42]. Based on the model for a system of charged dipolar colloids or proteins presented by Phillies [43] and Bratko *et al* [29, 30], the energy required to form an aggregate of a certain shape from its constituent particles located at infinite separation (W_{total}) was approximated as a sum of the Coulombic charge–charge, charge–dipole, dipole–dipole interactions and the Van der Waals interaction. All the interaction potentials were dependent on the mutual geometric configuration of the system:

$$W_{\text{total}}(r,\theta,\phi) = W_{q-q}(r) + W_{q-\mu}(r,\theta) + W_{\mu-q}(r,\theta) + W_{\mu-\mu}(r,\theta,\varphi) + W_{\text{Van der Waals}}(r). \tag{2}$$

The potential arising from net charge and dipole contributions may be calculated as [43]

$$W(r) = \frac{q_i q_j}{4\pi\varepsilon_0\varepsilon r_{ij}} e^{-kr_{ij}} C_0^2 + 2\frac{q_i\mu_j\cos(\theta_j)}{4\pi\varepsilon_0\varepsilon r_{ij}^2} e^{-kr_{ij}}(1-kr_{ij})C_0C_1 + \frac{\mu_i\mu_j}{4\pi\varepsilon_0\varepsilon r_{ij}^3}(\cos(\theta_i)\cos(\theta_j) \times[2+2kr_{ij}+(2kr_{ij})^2] + \sin(\theta_i)\sin(\theta_j)\cos(\phi_i-\phi_j)[1+kr_{ij}])e^{-kr_{ij}}C_1^2, \tag{3}$$

where

$$C_0 = \frac{e^{ka}}{1+ka}; \qquad C_1 = \frac{3e^{ka}}{[2+2ka+(ka)^2+(1+ka)/\ni]}.$$

Here, θ_i is defined as an angle between the dipole vector $\vec{i}$ and the vector $\vec{r}$ connecting the centres of the particles, $0 < \theta < 2\pi$, φ_i is the angle describing the rotation of dipole around $\vec{r}$, $0 < \varphi < \pi$, and r is the distance between two particles. $1/k$ is the Debye screening length, ε_0 the permittivity of vacuum, ε the effective permittivity of the medium, which was approximated as a function of interparticle distance by the use of the logarithmic composite mixing rule [44].

The Hamaker molecular model of London–Van der Waals forces was used in the simulation [45, 46]. The dispersion interaction energy for two equal sized spherical particles with radius r and a centre-to-centre distance R in this model is given as [47]

$$W_{\text{Van der Waals}}(r) = -\frac{A_{121}}{6}\left\{\frac{2r^2}{R^2-4r^2} + \frac{2r^2}{R^2} + \ln\left[1-\frac{4r^2}{R^2}\right]\right\}, \tag{4}$$

where A_{121} is the Hamaker constant. The value for a closely related semiconductor, CdS, interacting across water, was used as the actual value ($A = 4.85\times10^{-20}$ J) [47]. No adjustment of the Hamaker constant value for size dependent NP properties was necessary since the interatomic distances for both CdTe and CdS NPs in the size regime considered here (3–5 nm) do not differ excessively from the bulk values [48, 49], and, therefore, neither do their dielectric properties nor the Hamaker constant [50]. Since at distances where retardation becomes relevant (>5 nm), the electrostatic repulsion between similarly charged NPs outweighs the dispersion attraction, retarded interactions were not considered.

2.3. Linearity coefficient

In order to be able to analyse and compare the geometrical layouts of the resulting configurations, as applied to the degree of linearity, we used such values as the average interparticle distance, the number of nearest neighbours for each particle and a linear length coefficient that was calculated as the ratio between the maximum possible one-dimensional length of a chain of N particles and the actual distance between two most distant particles in the simulated system.

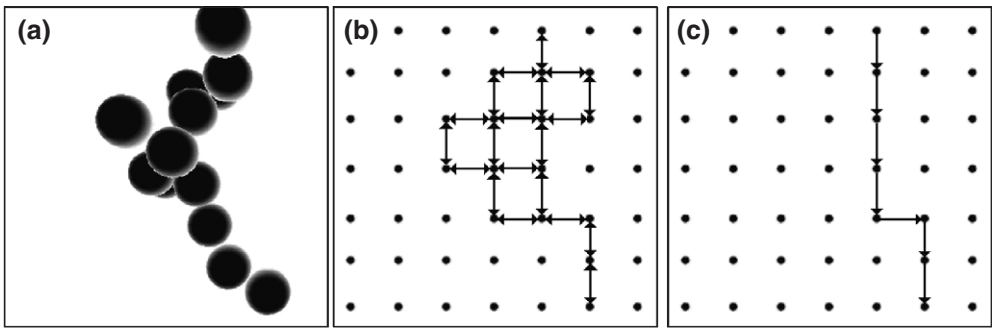

Figure 3. Calculation of the linearity coefficient. The original system (*a*), All-Pairs-Shortest-Paths (*b*) and the shortest path between two most distant particles (*c*).

The following algorithm, based on graph theory [51], was used in its calculation. First, the system structure (figure 3(*a*)) was represented as a connected, undirected graph G defined as a pair $G = (V, E)$, where V is a set of vertices and E is a set of edges between the vertices. The undirected graph G was considered as a directed graph with two directed edges for each undirected edge and was represented by the adjacency matrix W with the edges weighted equal to one. The adjacency of the edges was calculated according to whether particle i and particle j are neighbours or not, i.e. $d(i, j) < \delta$. Then, the Floyd–Warshall All-Pairs-Shortest-Path [52] algorithm was used to solve the shortest-path problem by means of an adjacency matrix (figure 3(*b*)):

$$f_{ij}(k) = \begin{cases} w_{ij}, & \text{if } k < 0, \\ \min\left(f_{ij}(k-1),\, f_{ik}(k-1) + f_{ki}(k-1)\right), & \text{if } k > 0, \end{cases} \tag{5}$$

where w_{ij} is a (i, j) cell of adjacency matrix W and $f_{ij}(k)$ is a i, j value from a Floyd–Warshall minimum distances matrix. Finally, the minimum distances matrix is calculated and the ratio between the maximum value of f_{ij} and the number of particles in the system gives the final coefficient:

$$K_{\mathrm{G}} = \frac{\max(f_{ij})}{N} \times 100, \tag{6}$$

where N is the number of particles in the simulated system. Physically, this coefficient represents how far apart the two particles are that have the longest path from all the possible shortest paths between them in the simulated system (figure 3(*c*)), compared to an 'ideal' situation where all the particles are arrayed in a single line.

3. Results

Several series of NP aggregation simulations with different system parameters, summarized in table 1, were carried out. The influence of the dipole, the net charge and the size of the NP on the aggregation behaviour, was considered to be of major interest.

The results of the simulation show that the aggregation patterns of the NPs and the linearity of the NP clusters depend, to a greater or lesser extent, on all the investigated parameters.

Figure 4 shows simulation results for a system of 50 NPs with dipole values 0, 25, 100 and 400 D. From these pictures it is possible to assess visually, how the geometrical layout of the aggregates changes with increasing dipole moment strength. It is evident that the presence

Table 1. System parameters for different series of simulation runs.

System parameters	Dipole influence	Charge influence	Large N
Box size	$[20R \times 20R \times 20R]$	$[20R \times 20R \times 20R]$	$[70R \times 70R \times 70R]$
Number of particles, N	50	50	300–600
Particle diameter	4.4 nm	4.4 nm	4.4 nm
Net charge	$-1e^0$	$0–5e^0$	$-1e^0$
Net dipole	0–400 D	100 D	100 D

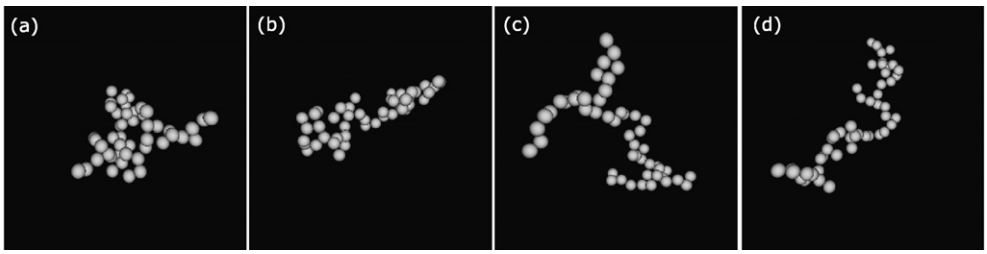

Figure 4. Simulation results for a system of 50 NPs with a charge of −1e and dipole values of: 0 (*a*), 25 D (*b*), 100 D (*c*) and 400 D (*d*).

of a dipole favours a more linear or chain-like form for the resulting configurations, especially at high dipole values.

In order to investigate the dependence of the system configuration on the dipole moment (*a*) and net charge (*b*) and (*c*) of the NPs, figure 5, the simulation results were averaged over 20 simulation runs for each particular system configuration, and the coefficient of linearity K_G described earlier was analysed. The unbiased estimation of the standard deviation $S_a = \sqrt{1/(n-1)\sum (x_i - m_a)^2}$ was used as a measure of the dispersal in a group of linearity coefficients, and a percentage representation of the coefficient of variation $CV = S_a/m_a \times 100\%$ was used to measure the relative variability of the linearity coefficient within similar simulation runs, where m_a is the mean value of the set and n is the number of runs. A total of 220 simulation tests was conducted for different parameter sets from table 1. It was found that the coefficient of variation of the linearity coefficient K_G ranged from 7.1% to 11.2%, with an overall average of 9.85%. Figure 5(*a*) shows K_G as a function of the particle dipole value at a fixed charge of −1e. Considering the statistical error margins, it can be seen that the dependence of K_G on the dipole is not very pronounced. While higher dipole values (400 D) certainly seem to enhance the linearity of the aggregates, the influence of the dipole is small in the range of experimentally found NP dipole values [15, 16]. The NP charge has also been found to influence the linearity coefficient. Figures 5(*b*) and (*c*) show the dependence of K_G on the charge at a dipole value of 100 D and 400 D, respectively. It can be seen that an increase of the charge leads to an increase in linearity in both cases, although the profile of the dependence is slightly different.

For an assessment of the similarity between the simulated configurations and the experimental TEM photographs of NP pearl-necklace aggregates from the work of Tang *et al* [13], a simulation of a system containing a relatively large number of particles (300) was performed. Figure 6 shows the resulting aggregate from two different viewpoints. It can be seen that in comparison to the experimental pictures the simulated aggregates have far more defects. Very few if any of the long, highly linear, single-particle 'pearl-necklace' chains that are observed

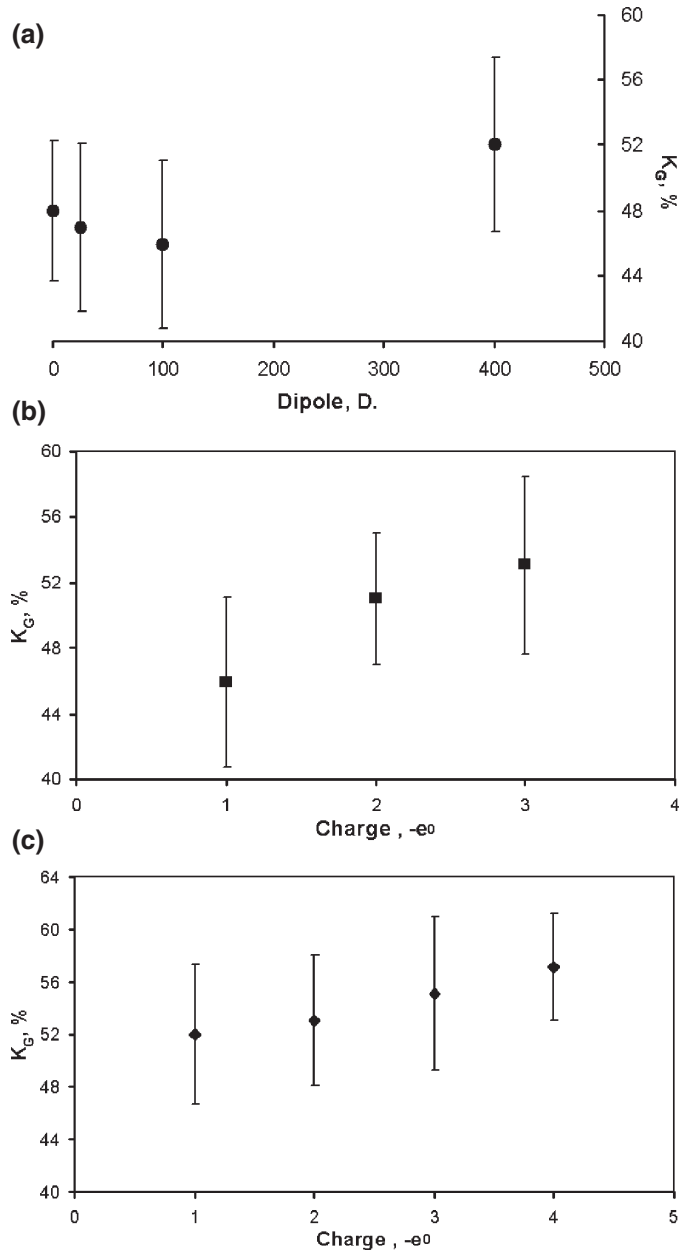

Figure 5. Linearity coefficient K_G (see text) as a function of: NP dipole at fixed charge (-1e) (*a*), and net charge at two different dipole values 100 D (*b*) and 400 D (*c*).

in the experiment are formed during the simulation. Of course, one other point that should be kept in mind when comparing three-dimensional simulated pictures with TEM photographs, is that during TEM measurements the system is forced into a planar two-dimensional state by the drying of the solvent, a process that may influence the final shape. The calculation of the linear coefficient K_G from TEM images of Tang *et al* [13] gives a range of values from 78.46 to 87.54, while the maximum value of K_G for the simulated 300 particles systems was 61.22. Thus, while

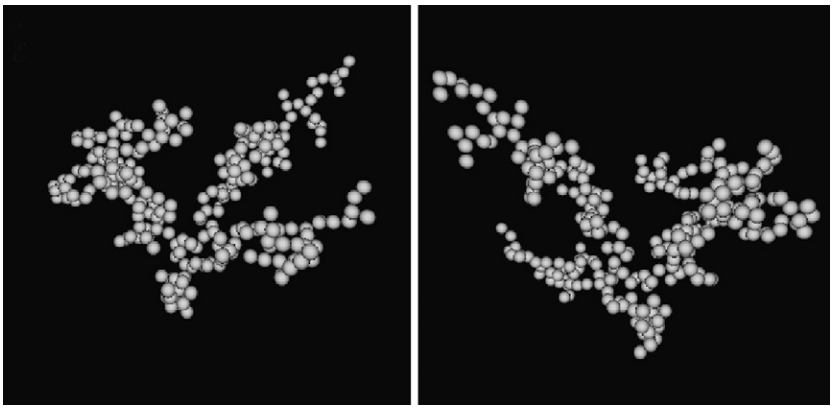

Figure 6. An aggregate of 300 NPs as viewed from two different points.

the current model can provide a rough estimate of the geometry of NP aggregates as a function of the parameters of the interacting particles, it has its deficiencies in that it does not take into account all the forces that act between the CdTe NPs in the experiment. While charge–dipole and dipole–dipole interactions are certainly very important for the process of NW self-assembly, it seems that, in addition, other, probably short-range interparticle forces, are responsible for organizing and holding together long and stable NP chains.

4. Conclusion

A model for the calculation of the interaction of semiconductor NPs and their aggregation into clusters has been developed. A 'linearity coefficient' has been introduced into the model that allows for the comparison of NP aggregate geometries and investigation of the dependence of aggregate shapes on NP charge and dipole strength. The described linearity coefficient K_{G} can serve as a powerful tool to investigate the influence of variable parameters, such as the dipole moment, net charge, NP sizes, etc on the final system configuration from the point of view of its affinity to the linear structure. Computer simulations, based on this model, showed that aggregates with varying degrees of linearity can be formed if the values for the NP charge and dipole that are used are in the range of those found experimentally. However, the simulated aggregate shapes are different from those seen in the experiment as regards the length and number of defects. The inclusion in the model of further forces acting between NPs in solution could possibly increase its reliability in predicting aggregate shapes. This modelling approach can be applied to the study of the aggregation of different kinds of NPs, although currently CdTe NPs are the only species that have been experimentally found to form extended pearl-necklace chain networks.

References

[1] Alivisatos A P 1996 Semiconductor clusters, nanocrystals, and quantum dots *Science* **271** 933–7
[2] Coe S, Woo W K, Bawendi M and Bulovic V 2002 Electroluminescence from single monolayers of nanocrystals in molecular organic devices *Nature* **420** 800–3
[3] Duan X F, Huang Y, Agarwal R and Lieber C M 2003 Single-nanowire electrically driven lasers *Nature* **421** 241–5

[4] Pientka M, Wisch J, Boger S, Parisi J, Dyakonov V, Rogach A, Talapin D and Weller H 2004 Photogeneration of charge carriers in blends of conjugated polymers and semiconducting nanoparticles *Thin Solid Films* **451–452** 48–53
[5] Xia Y N, Yang P D, Sun Y G, Wu Y Y, Mayers B, Gates B, Yin Y D, Kim F and Yan Y Q 2003 One-dimensional nanostructures: synthesis, characterization, and applications *Adv. Mater.* **15** 353–89
[6] Weller H 2003 Synthesis and self-assembly of colloidal nanoparticles *Phil. Trans. R. Soc. Lond. Ser. A: Math. Phys. Eng. Sci.* **361** 229–39
[7] Kelly J M, O'Brien P, Weller H, Green M and Harding J H 2003 New synthetic routes for quantum dots—discussion *Phil. Trans. R. Soc. Lond. Ser. A: Math. Phys. Eng. Sci.* **361** 310
[8] Peng X G, Manna L, Yang W D, Wickham J, Scher E, Kadavanich A and Alivisatos A P 2000 Shape control of CdSe nanocrystals *Nature* **404** 59–61
[9] Lu X M, Hanrath T, Johnston K P and Korgel B A 2003 Growth of single crystal nanowires in supercritical silicon solution from tethered gold particles on a silicon substrate *Nano Lett.* **3** 93–9
[10] Yu H and Buhro W E 2003 Solution–liquid–solid growth of soluble GaAs nanowires *Adv. Mater.* **15** 416–9
[11] Kan S, Mokari T, Rothenberg E and Banin U 2003 Synthesis and size-dependent properties of zinc-blende semiconductor quantum rods *Nature Mater.* **2** 155–8
[12] Yin M, Gu Y, Kuskovsky I L, Andelman T, Zhu Y, Neumark G F and O'Brien S 2004 Zinc oxide quantum rods *J. Am. Chem. Soc.* **126** 6206–7
[13] Tang Z Y, Kotov N A and Giersig M 2002 Spontaneous organization of single CdTe nanoparticles into luminescent nanowires *Science* **297** 237–40
[14] Tang Z Y, Ozturk B, Wang Y and Kotov N A 2004 Simple preparation strategy and one-dimensional energy transfer in CdTe nanoparticle chains *J. Phys. Chem.* B **108** 6927–31
[15] Blanton S A, Leheny R L, Hines M A and Guyot-Sionnest P 1997 Dielectric dispersion measurements of CdSe nanocrystal colloids: observation of a permanent dipole moment *Phys. Rev. Lett.* **79** 865–8
[16] Shim M and Guyot-Sionnest P 1999 Permanent dipole moment and charges in colloidal semiconductor quantum dots *J. Chem. Phys.* **111** 6955–64
[17] Rabani E 2001 Structure and electrostatic properties of passivated CdSe nanocrystals *J. Chem. Phys.* **115** 1493–7
[18] Gavartin J L and Stoneham A M 2003 Quantum dots as dynamical systems *Phil. Trans. R. Soc. Lond. Ser. A: Math. Phys. Eng. Sci.* **361** 275–89
[19] Rabani E, Hetenyi B, Berne B J and Brus L E 1999 Electronic properties of CdSe nanocrystals in the absence and presence of a dielectric medium *J. Chem. Phys.* **110** 5355–69
[20] Liao J H, Zhang Y, Yu W, Xu L N, Ge C W, Liu J H and Gu N 2003 Linear aggregation of gold nanoparticles in ethanol *Colloids Surf. A: Physicochem. Eng. Aspects* **223** 177–83
[21] Chang J Y, Chang J J, Lo B, Tzing S H and Ling Y C 2003 Silver nanoparticles spontaneous organize into nanowires and nanobanners in supercritical water *Chem. Phys. Lett.* **379** 261–7
[22] Cha J N, Birkedal H, Euliss L E, Bartl M H, Wong M S, Deming T J and Stucky G D 2003 Spontaneous formation of nanoparticle vesicles from homopolymer polyelectrolytes *J. Am. Chem. Soc.* **125** 8285–9
[23] Euliss L E, Grancharov S G, O'Brien S, Deming T J, Stucky G D, Murray C B and Held G A 2003 Cooperative assembly of magnetic nanoparticles and block copolypeptides in aqueous media *Nano Lett.* **3** 1489–93
[24] Murthy V S, Cha J N, Stucky G D and Wong M S 2004 Charge-driven flocculation of poly(L-lysine)-gold nanoparticle assemblies leading to hollow microspheres *J. Am. Chem. Soc.* **126** 5292–9
[25] Wong M S, Cha J N, Choi K S, Deming T J and Stucky G D 2002 Assembly of nanoparticles into hollow spheres using block copolypeptides *Nano Lett.* **2** 583–7
[26] Cho K S, Gaschler W L, Murray C B and Stokes K L 2002 PBSE nanocrystals, nanowires and superlattices *Abstracts of Papers of the American Chemical Society* vol 224, p U308
[27] Pacholski C, Kornowski A and Weller H 2002 Self-assembly of ZnO: from nanodots to nanorods *Abstracts of Papers of the American Chemical Society* vol 224, p U351
[28] Wu J Z, Bratko D, Blanch H W and Prausnitz J M 1999 Monte Carlo simulation for the potential of mean force between ionic colloids in solutions of asymmetric salts *J. Chem. Phys.* **111** 7084–94
[29] Striolo A, Bratko D, Wu J Z, Elvassore N, Blanch H W and Prausnitz J M 2002 Forces between aqueous nonuniformly charged colloids from molecular simulation *J. Chem. Phys.* **116** 7733–43
[30] Bratko D, Striolo A, Wu J Z, Blanch H W and Prausnitz J M 2002 Orientation-averaged pair potentials between dipolar proteins or colloids *J. Phys. Chem.* B **106** 2714–20
[31] Tej M K and Meredith J C 2002 Simulation of nanocolloid chemical potentials in a hard-sphere polymer solution: expanded ensemble Monte Carlo *J. Chem. Phys.* **117** 5443–51
[32] Lu X J and Kindt J T 2004 Monte Carlo simulation of the self-assembly and phase behavior of semiflexible equilibrium polymers *J. Chem. Phys.* **120** 10328–38

[33] Wittmer J P, Milchev A and Cates M E 1998 Dynamical Monte Carlo study of equilibrium polymers: static properties *J. Chem. Phys.* **109** 834–45
[34] Tsonchev S, Schatz G C and Ratner M A 2004 Electrostatically-directed self-assembly of cylindrical peptide amphiphile nanostructures *J. Phys. Chem.* B **108** 8817–22
[35] Richter J, Adler M and Niemeyer C M 2003 Monte Carlo simulation of the assembly of bis-biotinylated DNA and streptavidin *Chemphyschem* **4** 79–83
[36] Metropolis N, Rosenbluth A W, Rosenbluth M N, Teller A H and Teller E 1953 Equation of State Calculations by Fast Computing Machines *J. Chem. Phys.* **21** 1087–92
[37] Blair M J and Patey G N 1998 Gas–liquid coexistence and demixing in systems with highly directional pair potentials *Phys. Rev.* E **57** 5682–6
[38] Stevens M J and Grest G S 1995 Structure of soft-sphere dipolar fluids *Phys. Rev.* E **51** 5962–75
[39] Stevens M J and Grest G S 1994 Coexistence in dipolar fluids in a field *Phys. Rev. Lett.* **72** 3686–9
[40] Davis S W, McCausland W, McGahagan H C, Tanaka C T and Widom M 1999 Cluster-based Monte Carlo simulation of ferrofluids *Phys. Rev.* E **59** 2424–8
[41] Derjaguin B and Landau L 1945 Theory of stability of highly charged liophobic sols and adhesion of highly charged particles in solutions of electrolytes *Zh. Eksp. Teor. Fiz.* **15** 663–82
[42] Verwey E J W, Overbeek J T and Nes Kv 1948 *Theory of the Stability of Lyophobic Colloids the Interaction of Sol Particles Having an Electric Double Layer* (New York: Elsevier)
[43] Phillies G D 1974 Excess chemical potential of dilute-solutions of spherical polyelectrolytes *J. Chem. Phys.* **60** 2721–31
[44] Habeger C F, Condon C E, Khan S R and Adair J H 1997 Evaluation of the calcium oxalate monohydrate Hamaker constant based on static dielectric constant determination and electronic polarization *Colloids Surf B: Biointerfaces* **10** 13–21
[45] Hamaker H C 1937 The London–Van-der-Waals attraction between spherical particles *Physica (Utrecht)* **4** 1058–72
[46] Wang S P, Mamedova N, Kotov N A, Chen W and Studer J 2002 Antigen/antibody immunocomplex from CdTe nanoparticle bioconjugates *Nano Lett.* **2** 817–22
[47] Morrison I D and Ross S 2002 *Colloidal Dispersions, Suspensions, Emulsions and Foams* (New York: Wiley)
[48] Rockenberger J, Troger L, Kornowski A, Vossmeyer T, Eychmuller A, Feldhaus J and Weller H 1997 EXAFS studies on the size dependence of structural and dynamic properties of CdS nanoparticles *J. Phys. Chem.* B **101** 2691–701
[49] Rockenberger J, Troger L, Rogach A L, Tischer M, Grundmann M, Weller H and Eychmuller A 1998 An EXAFS study on thiolcapped CdTe nanocrystals *Ber. Bunsenges—Phys. Chem. Chem. Phys.* **102** 1561–4
[50] Lifshitz E M 1956 The theory of molecular attractive forces between solids *Sov. Phys.—JETP-USSR* **2** 73–83
[51] Gross J L and Yellen J 1999 *Graph Theory and its Applications* (Boca Raton, FL: CRC Press)
[52] Cormen T H, Leiserson C E and Rivest R L 1990 *Introduction to Algorithms* (Cambridge, MA: MIT Press)